

0038-1098(94)00337-8

CRITICAL HELIUM CONCENTRATION AND ITS EFFECT ON
BUBBLE GROWTH IN PALLADIUM

R. Rajaraman, B. Viswanathan and K.P. Gopinathan

Materials Science Division, Indira Gandhi Centre for Atomic Research, Kalpakkam 603 102, India

(Received 7 March 1994 by C.N.R. Rao)

Helium bubble growth in palladium, implanted with different helium concentrations from 25 to 250 appm, has been investigated by positron lifetime spectroscopy during isochronal annealing. It is found that the bubble growth behaviour for helium above a critical concentration of 100 appm is different from that for doses below it. In palladium with <100 appm helium, the bubble radius increases sharply with annealing temperature. For helium concentrations ≥ 100 appm, the bubble radius increases slowly upto 1200 K, above which the growth rate picks up. These observations are explained on the basis of the build-up of over-pressure in bubbles and correlating the change in growth behaviour with pressure.

1. INTRODUCTION

INERT gases such as helium, being extremely insoluble in metals, tend to precipitate into bubbles. A comprehensive study of the behaviour of inert gases in metals has been a topic of intensive research over the years [1, 2]. Helium accumulation in structural materials used in fission and fusion reactor environments is of technological importance, since it leads to degradation of mechanical properties [3]. Studies of helium in metal tritides such as palladium tritide are also of importance, as these tritides are used in storage of tritium and helium is produced by the radioactive decay of tritium [4]. A key parameter governing bubble growth is the pressure inside bubbles [1, 5]. Evidence for over-pressure in bubbles, in excess of equilibrium pressures has been reported in post-implantation annealing of Ni by small angle neutron scattering [6] and positron annihilation measurements [7]. The over-pressure and its variation with annealing temperature and time are found to influence helium bubble growth mechanism and kinetics in Pd [8, 9]. From a systematic analysis of TEM studies of helium bubbles in Ni, based on the compilation of results from various investigations, interesting trends on bubble growth have been reported [10]. In that study, it was found that for annealing temperatures above 900 K, and for high He concentrations of

500-5000 appm, the bubble growth rate at regions close to the surface of the sample is substantially higher than that in the bulk, but it is comparable to the growth rate in the bulk at He concentrations <200 appm [10]. These observations have been explained by a model where a change in growth mechanism has been correlated with a change in pressure inside bubbles [5]. A suggestion for the existence of a critical helium concentration to build-up over-pressure in bubbles has been made [11]. A thermodynamic analysis of vacancy deficit conditions induced by over-pressure in bubbles has led to a relationship between the degree of vacancy deficit and bubble parameters [12]. The present work is aimed at providing unambiguous and direct evidence for the existence of a critical helium concentration for building up over-pressure and forming non-equilibrium bubbles. This study also addresses itself to the effect of helium dose around the critical helium concentration on bubble growth behaviour. Being defect specific and sensitive to helium clustering over a wide size range, positron lifetime spectroscopy gives information on helium atom density and thereby pressure, the average bubble radius and bubble concentration [13, 14]. The present work takes advantage of this, in making systematic and detailed positron lifetime measurements in Pd implanted with helium to different concentrations from 25 to 250 appm.

2. EXPERIMENTAL DETAILS

Well annealed Pd samples of purity 99.99% and of dimensions $10\text{ mm} \times 10\text{ mm} \times 250\text{ }\mu\text{m}$ were homogeneously implanted with helium over the entire sample depth by degrading the energy of 40 MeV α -particles from the Variable Energy Cyclotron at Calcutta. The irradiation temperature was maintained at $320 \pm 25\text{ K}$ for all the samples. A pair of samples each were implanted with 25, 50, 100, 150 and 250 appm He. Positron lifetime measurements were made on these samples in the as-implanted state and as a function of post-implantation isochronal (30 min) annealing temperature from 300 to 1523 K. A lifetime spectrometer of the fast-fast coincidence type having a prompt time resolution of 220 ps (FWHM) was used for the measurements. The measured spectra were analysed for the different lifetime components, τ_1 , τ_2 and their relative intensities I_1 , I_2 using the programmes RESOLUTION and POSITRONFIT [15].

3. RESULTS AND DISCUSSION

Figure 1a shows the variation of resolved lifetime components τ_1 , τ_2 and the intensity of the τ_2 component I_2 as a function of annealing temperature in Pd with 25 appm He. In the as-implanted state, the shorter lifetime, $\tau_1 = 170\text{ ps}$ with 98% intensity may be explained as due to small helium-vacancy complexes formed by the trapping of mobile vacancies by helium. The longer lifetime, $\tau_2 = 500\text{ ps}$ of 2% intensity is attributed to microvoids formed by the agglomeration of mobile vacancies. The low intensity microvoid component disappears at 523 K beyond which a single lifetime with 100% intensity is observed until 673 K. This is shown by filled squares in Fig. 1a. The reduction of τ_1 from an initial value of 170 to 160 ps at 673 K is indicative of helium decoration of the trapping sites leading to nucleation of bubbles [14]. A high concentration of bubble embryos stabilized upon annealing, can explain the observed saturation trapping of positrons corresponding to the single lifetime. Above 723 K, two lifetimes are again resolved: τ_2 associated with bubbles and τ_1 with the bulk state in accordance with the two state trapping model [16]. This signifies the bubble growth range. The marked increase in τ_2 towards saturation is brought about by the reduction of helium density inside bubbles during growth while the reduction of I_2 arises from the decrease in the number density of growing bubbles. The annealing features for Pd with 50 appm He (figure not shown) are found to be similar to those for Pd with 25 appm He. Figure 1b

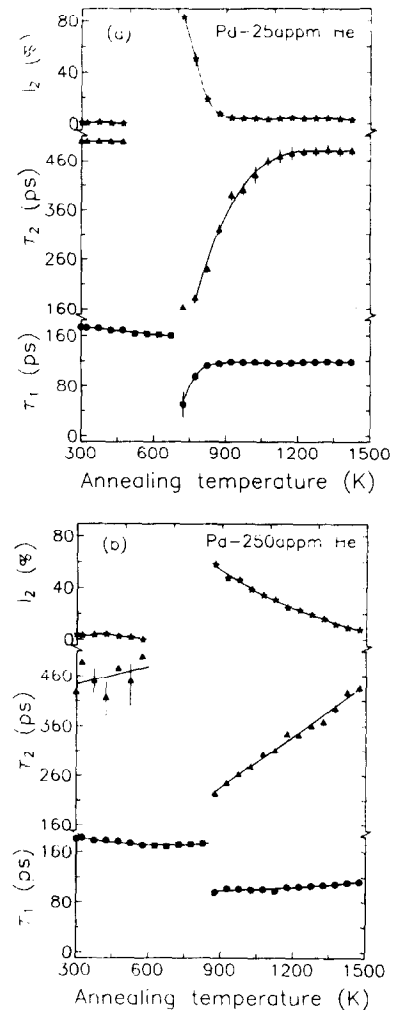


Fig. 1. Variation of the resolved positron lifetime parameters with annealing temperature in (a) Pd with 25 appm He and (b) Pd with 250 appm He. The filled squares correspond to the single lifetime of intensity 100% in the temperature range shown.

shows the variation of the resolved lifetime parameters for Pd with a higher helium concentration of 250 appm. The lifetime behaviour for the sample with 250 appm He in the initial annealing range is similar to that for Pd with 25 appm He. But, the variation of τ_2 and I_2 in the growth region for 250 appm He exhibits features different from those for 25 appm He (cf. Figs. 1a and 1b). The annealing features of lifetime for Pd with 150 appm He, over the entire temperature range are found to be similar to those of Pd with 250 appm He and these in turn are similar to those for Pd with 100 appm He reported earlier [8]. Based on the comparison of lifetime behaviour in samples with different helium concentrations (25–250 appm), the following observations are made:

(a) The temperature of the onset of bubble growth shifts upward with increasing helium concentration. While the onset of bubble growth is ~ 700 K for Pd with 25 appm He, it is ~ 900 K for Pd with 250 appm He.

(b) The bubble growth behaviour, as judged from the nature of variation of τ_2 and I_2 falls into two patterns. For low dose samples (25 and 50 appm He), τ_2 increases sharply and then tends towards saturation. This is accompanied by a sharp reduction of I_2 . In the high dose (100–250 appm He) samples the increase of τ_2 and decrease of I_2 are rather monotonic without showing any saturation. The latter observation suggests the existence of a critical helium concentration at which the bubble growth behaviour changes.

In order to study in detail the effect of the critical helium concentration on bubble growth, the bubble parameters, viz. the helium atom density n_{He} , the average bubble radius R_b and bubble concentration C_b , have been extracted from an analysis of experimental lifetime parameters using the procedure reported earlier [8, 14]. A positron lifetime–gas density relation proposed earlier on the basis of the positron surface state model [17] for bubbles can be generalized to most of the metal–helium systems to a first approximation. Accordingly, n_{He} is obtained from the values of the experimental lifetime τ_2 . The positron trapping rate in bubbles is known from the measured lifetime parameters. Using these, a helium inventory equation is set up and solved to obtain R_b and hence C_b [8, 14]. The satisfactory agreement between the bubble radius so deduced in He-implanted Pd [8] with that from direct TEM observations [18] validates the above mentioned analysis scheme. The helium pressure P_b in the bubbles has been computed from the experimental value of n_{He} using Trinkaus' equation of state [19].

The variation of the deduced helium pressure as a function of the bubble radius is shown in Fig. 2 for different implanted He concentrations. The equilibrium bubble pressures, as estimated from $P_{\text{eq}} = 2\gamma/R_b$, where γ is the surface energy (1.6 N m^{-1} for Pd [20]), are shown as the solid line in Fig. 2 for comparison. For the cases of Pd with 25 and 50 appm He, the bubble pressures are slightly higher than the equilibrium values in the initial size range, but the pressures match with the equilibrium curve for bubble radii > 10 nm. In sharp contrast to this, there is a significant over-pressure in excess of equilibrium pressures in the initial size range for samples with 100, 150 and 250 appm He. This over-pressure does not relax to equilibrium values even in bubbles of radii in the range of 15–20 nm for higher

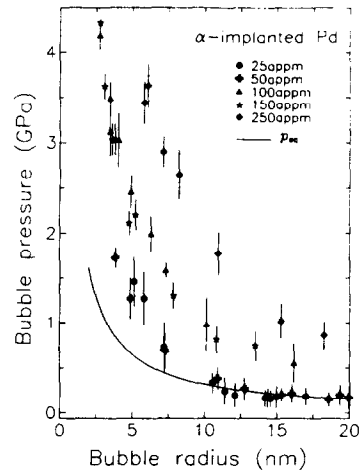


Fig. 2. Variation of the deduced bubble pressure with bubble radius for Pd containing 25, 50, 100, 150 and 250 appm He. The solid line corresponds to equilibrium pressures.

doses of He. The above observations are understood as follows: Over-pressurized bubbles readily absorb the available vacancies, resulting in conditions of vacancy deficit in the region around them. The resulting gradient in vacancy concentration sets-up a flow of vacancies from sources such as sample surface and grain boundaries. However, the net vacancy flow to the matrix interior at a given temperature will be determined by the concentration of over-pressurized bubbles close to vacancy sources as these bubbles effectively shield other bubbles far away from the sources [21]. This, coupled with the fact that the overall bubble concentration in the high dose samples is large, results in vacancy-deficient environment leading to inadequate relaxation of the over-pressure in bubbles. On the other hand, in samples with 25 and 50 appm He, the relatively lower over-pressure and smaller concentration of bubbles in the initial stages of annealing, result in adequate vacancy supply to relax bubble pressures to equilibrium values. It is thus clear that a critical helium concentration of ~ 100 appm is necessary to build sufficient over-pressure and form non-equilibrium bubbles, whose growth depends on the conditions of vacancy deficit. Figure 3 shows bubble growth curves in the form of variation of R_b with annealing temperature for Pd with different implanted helium concentrations (25–250 appm). As seen from the figure, the bubble radius increases sharply with annealing temperature over the entire annealing range for Pd with 25 and 50 appm He. On the other hand, for samples with 100, 150 and 250 appm He, the growth is slower in the temperature interval upto 1200 K as compared to that in samples with lower helium concentrations. The growth rate

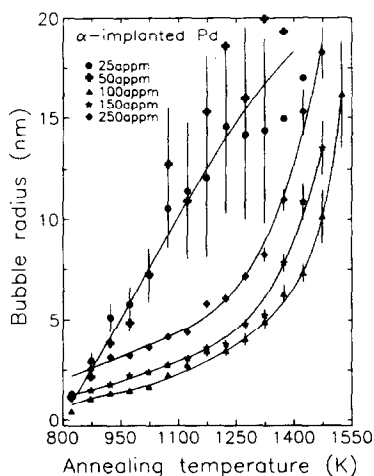


Fig. 3. Variation of the deduced bubble radius with annealing temperature for Pd with different helium concentrations indicated. The solid lines are guides for the eye.

picks up with a different slope above 1200 K. Complementary features with different growth branches have been seen in the variation of the deduced bubble concentration C_b for samples with low and high He concentrations as shown in Fig. 4. Within the framework of the surface diffusion controlled bubble migration and coalescence model, the observed behaviour in Fig. 3 may be qualitatively explained by correlating the pressure inside bubbles with bubble diffusivity [8, 9]. For Pd with helium concentration equal to or greater than the critical helium concentration, the high overpressure in the bubbles suppresses bubble diffusivity resulting in inhibited coalescence in the growth stage. This leads

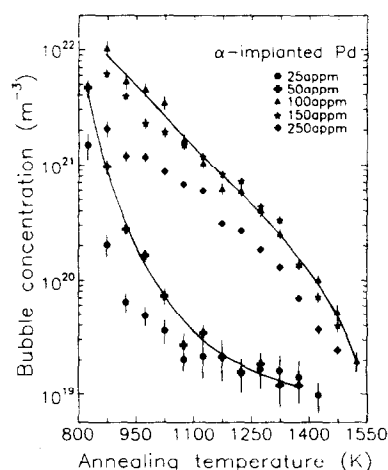


Fig. 4. Variation of helium bubble concentration in Pd with annealing temperature. The solid lines drawn for data corresponding to 50 and 100 appm helium are for guidance for the eye.

to lower growth rate in the initial annealing range upto 1200 K. At higher annealing temperatures, relaxation of overpressure, though not to equilibrium values, favours enhanced bubble diffusivity leading to faster growth as seen in Fig. 3. In the case of Pd with helium concentrations lower than the critical concentration, over the entire annealing range, bubble diffusion is not inhibited because of the prevalence of equilibrium or near-equilibrium pressures. This results in faster growth as observed in Fig. 3. It may, however, be mentioned that for low helium dose samples, the contribution of Ostwald ripening mechanism to explain the fast growth at equilibrium pressures is not ruled out [10]. But Ostwald ripening is completely suppressed at high internal pressures corresponding to high dose samples [5].

4. CONCLUSIONS

From positron lifetime measurements made on Pd implanted with different helium concentrations in the range of 25–250 appm, bubble pressures, average bubble radii and bubble concentrations have been deduced at different annealing temperatures. There is clear evidence for the existence of a critical helium concentration of ~ 100 appm to build sufficient overpressure in bubbles and form non-equilibrium bubbles which grow under conditions of vacancy deficit. The critical helium concentration has a marked influence on the bubble growth behaviour. For helium doses equal to or greater than the critical helium concentrations, pressure impeded bubble diffusivity results in the inhibition of coalescence leading to slower growth in the initial region of overpressure. Upon further annealing, relaxation of overpressure enhances bubble diffusion resulting in an increase of growth rate. For helium doses below the critical concentration of 100 appm, bubble growth is not inhibited by pressure throughout the annealing range and fast growth results. In conclusion, the present results provide an unambiguous and independent confirmation of the existence of a critical helium concentration and its influence on helium bubble growth in metals.

Acknowledgements – The authors thank Dr G. Amarendra for help during helium implantation runs and Dr C.S. Sundar for critical comments on the manuscript.

REFERENCES

1. See, for example, *Fundamental Aspects of Inert Gases in Solids*, (Edited by S.E. Donnelly & J.H. Evans), NATO Advanced Study Institute, Series B, Vol. 279, Plenum, New York (1991).

2. See, for example, *Fundamental Aspects of Helium in Metals* (Edited by H. Ullmaier), Proceedings of the International Symposium, Julich, Germany (1982); see *Radiat. Eff.* **78** (1983).
3. H. Ullmaier, *Nucl. Fusion* **24**, 1039 (1984).
4. M.S. Ortman, L.K. Heung, A. Nobile & R.L. Rabun, *J. Vac. Sci. Technol.* **A8**, 2881 (1990).
5. H. Trinkaus, *Scripta Metall.* **23**, 1773 (1989).
6. H. Ullmaier, in Ref. 1, p. 277.
7. B. Viswanathan & G. Amarendra, in Ref. 1, p. 209.
8. R. Rajaraman, G. Amarendra, B. Viswanathan & K.P. Gopinathan, *Phil. Mag. Lett.* **68**, 257 (1993).
9. R. Rajaraman, B. Viswanathan, M.C. Valsakumar & K.P. Gopinathan, *Phys. Rev.* **B50** (1994) (in press).
10. V.N. Chernikov, H. Trinkaus, P. Jung & H. Ullmaier, *J. Nucl. Mater.* **170**, 31 (1990).
11. V.N. Chernikov, P.R. Kazansky, H. Trinkaus, P. Jung & H. Ullmaier, in Ref. 1, p. 329.
12. S.L. Kanashenko & V.N. Chernikov, *J. Nucl. Mater.* **195**, 260 (1992).
13. K.O. Jensen, M. Eldrup, B.N. Singh & M. Victoria, *J. Phys.* **F18**, 1069 (1988).
14. G. Amarendra, B. Viswanathan, A. Bharathi & K.P. Gopinathan, *Phys. Rev.* **B45**, 10231 (1992).
15. P. Kirkegaard, M. Eldrup, O.E. Mogensen & N.J. Pedersen, *Comput. Phys. Commun.* **23**, 307 (1981).
16. See, for example, R.N. West, in *Positrons in Solids*, (edited by P. Hautojarvi), p. 89, Springer, New York (1979).
17. K.O. Jensen & R.M. Nieminen, *Phys. Rev.* **B35**, 2087 (1987); **B36**, 8219 (1987).
18. R. Rajaraman, *Positron Annihilation Studies of Light Impurities in Metals*, Ph.D thesis, University of Madras, Madras, October 1993 (unpublished).
19. H. Trinkaus, *Radiat. Eff.* **78**, 189 (1983).
20. E.A. Brandes, *Smithalls Metals Reference Book*, p. 14.8. Butterworths, London (1983).
21. N. Marcochov, L.J. Perryman & P.J. Goodhew, *J. Nucl. Mater.* **149**, 296 (1987).